

EmotiCrafter: Text-to-Emotional-Image Generation based on Valence-Arousal Model

Yi He[†]
iDVX Lab, Tongji University
Shanghai, China
heyi.hy11@gmail.com

Shengqi Dang[†]
iDVX Lab, Tongji University
Shanghai, China
dangsq123@tongji.edu.cn

Long Ling
iDVX Lab, Tongji University
Shanghai, China
lucyling0224@gmail.com

Ziqing Qian
iDVX Lab, Tongji University
Shanghai, China
2411920@tongji.edu.cn

Nanxuan Zhao
Adobe Research
California, USA
nanxuanzhao@gmail.com

Nan Cao*
iDVX Lab, Tongji University
Shanghai, China
nan.cao@gmail.com

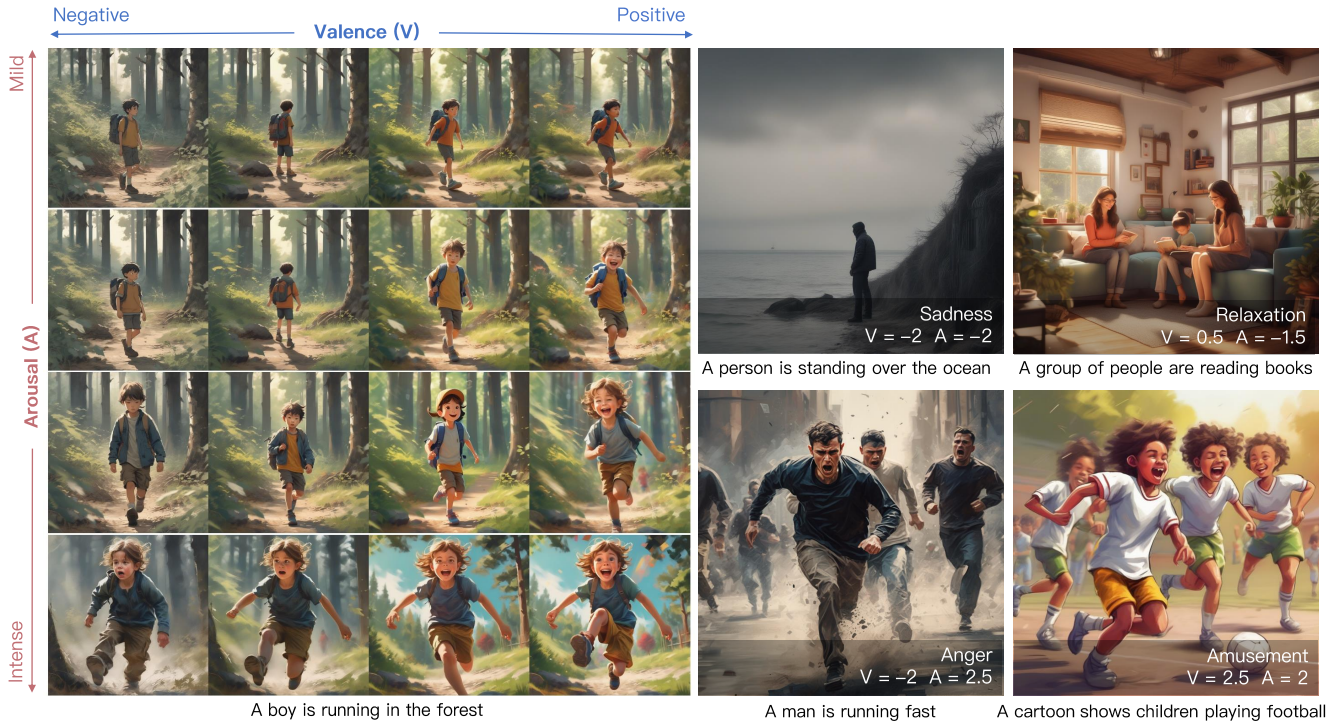


Figure 1. Generated images of the *EmotiCrafter*. Given a prompt and Valence-Arousal (V-A) values, our method can generate an emotional image that reflects the input prompt and aligns with the specified emotion values. By adjusting the V-A values, our method can also generate images that evoke discrete emotions, such as sadness, relaxation, anger, and amusement.

Abstract

Recent research shows that emotions can enhance users' cognition and influence information communication. While research on visual emotion analysis is extensive, limited work has been done on helping users generate emotionally rich image content. Existing work on emotional image

generation relies on discrete emotion categories, making it challenging to capture complex and subtle emotional nuances accurately. Additionally, these methods struggle to control the specific content of generated images based on text prompts. In this work, we introduce the new task of continuous emotional image content generation (C-EICG) and present *EmotiCrafter*, an emotional image generation model that generates images based on text

[†]Yi He and Shengqi Dang contributed equally to this work.

*Nan Cao is the corresponding author.

prompts and Valence-Arousal values. Specifically, we propose a novel emotion-embedding mapping network that embeds Valence-Arousal values into textual features, enabling the capture of specific emotions in alignment with intended input prompts. Additionally, we introduce a loss function to enhance emotion expression. The experimental results show that our method effectively generates images representing specific emotions with the desired content and outperforms existing techniques.

1. Introduction

Emotions are fundamental to human experiences and play a critical role in shaping how people perceive and interact with the world. Research has shown that emotions affect memory [5, 20, 24, 30, 47] and comprehension [21, 40, 42], which are crucial for effective communication. As a result, content creators increasingly recognize the importance of incorporating emotions to enhance audience engagement and comprehension.

While research on visual emotion analysis is extensive [18, 52, 61], there is limited work on generating emotionally rich image content. Some early studies explored emotion generation techniques within specific domains such as facial expressions [2, 48] or landscapes [29]. EmoGen [53] generates images based on a given emotion tag (e.g., happy or sad), which pioneered the domain-free emotional image generation (EICG) task. However, it has two critical limitations: (1) the image is generated from an emotion tag instead of a text prompt, making the generated content difficult to control; (2) While the discrete emotion tags used in EmoGen are easy to understand, psychologists have not achieved a consensus on the emotion categories [63]. The limited scope of discrete emotion tags falls short of capturing nuanced emotions. In contrast, the continuous emotion models represent emotions through a continuous Cartesian coordinate system, allowing for a more precise capture of emotional complexity and subtlety [2]. Therefore, developing a general text-to-image model that reflects continuous emotional variations is desired.

In this paper, we introduce the task of continuous emotional image content generation (C-EICG) and present *EmotiCrafter*, an emotional image generation model that generates images based on text prompts and V-A values (i.e., two real numbers $(v, a) \in [-3, +3]$) defined in the Valence-Arousal (V-A) emotion model [37], the most frequently used continuous emotional model in psychology. An emotion-embedding network is designed to embed V-A values into the text prompts of a stable diffusion XL model (SDXL) [32]. This network enables a nonlinear embedding of V-A values into the features of the input text prompt to capture complex emotional context for image generation. To train the model, a dataset with 39,843 annotated im-

ages is prepared. Given an image, a training sample consists of a pair of V-A values about the image labeled by human annotators and two prompts, i.e., neutral prompt and emotional prompt generated by GPT-4 based on the image. The neutral [emotion] prompt describes the essential content of the image, whereas the emotional prompt describes the emotional information, such as the color, light, and texture, about the image. Finally, to enhance the generation results, we introduce a loss function that normalizes the V-A distribution and scales the residuals between the features of the neutral and emotional prompts provided in each training sample. In summary, our contributions are as follows:

- We introduce a new task, i.e., continuous emotional image content generation (C-EICG), and propose a novel emotion-embedding network based on the transformer architecture. The network embeds the continuous Valence-Arousal values into the textual features of an input prompt for emotional image generation.
- We develop a novel loss function that helps to enhance the emotional resonance of generated images. The loss function modifies the target features to learn more obvious emotional changes and takes the V-A distribution into account to counter the unevenness of the data.
- We have constructed an emotional image dataset for training the proposed emotion-embedding network. Each training sample consists of a pair of unified V-A values, a neutral prompt, and an emotional prompt that are associated with the same image in the dataset.

2. Related work

In this section, we present a review of the related work, specifically focusing on visual emotion analysis, image emotion transfer, and conditional image generation.

2.1. Visual Emotion Analysis

Visual emotion analysis refers to the computational recognition and interpretation of human emotion [60] in visual media, such as images or videos. It has been a prominent research area, with most efforts focusing on the classification of discrete emotions [4, 44, 49, 51, 55]. However, discrete emotion categories limit the ability to capture the nuanced emotions [10], leading to an increased focus on continuous emotion analysis in images [62].

Much of the continuous emotion analysis remains centered on facial expression analysis [13, 15, 27, 39, 57]. While effective, facial analysis can overlook crucial contextual information that influences emotional interpretation. This drives studies to focus on emotions in objects or individuals within their environment, rather than just faces [16, 18, 18, 25, 26, 26]. For example, Kosti *et al.* [16] combined person-specific characteristics with the context of the scene to predict continuous emotional dimensions such

as arousal, valence, and dominance. Kragel *et al.* [18] proposed EmoNet to extract visual features such as facial expressions, body posture, and scene elements from images to predict valence and arousal values. Recently, Mertens *et al.* [26] tested multiple backbones (such as ResNet, CLIP, DINO, etc.) for prediction of valence and arousal, demonstrating strong performance across various architectures.

Previous studies have achieved high accuracy in predicting continuous emotions in images, demonstrating a correlation between continuous emotions and visual elements. Building on this insight, our work moves beyond prediction to explore how continuous emotions can be actively embedded within generated content. Specifically, we introduce the task of continuous emotional image content generation (C-EICG) and propose a novel emotion-embedding network.

2.2. Image Emotion Transfer

Image Emotion Transfer (IET) focuses on editing the content of the images to evoke different emotions [22, 31, 45, 64, 65]. For instance, Peng *et al.* [31] achieved emotion transfer by adjusting color tones and texture-related features. Zhu *et al.* [65] introduced a method that separates high-level emotion-relevant features (e.g., object shapes and scene layout) from low-level emotion-relevant features (e.g., brightness). By applying GANs, they transferred emotions between images while preserving their original structure. Building on these methods, Weng *et al.* [45] proposed the Affective Image Filter, which uses a multi-modal transformer to process both text and image inputs. With the emergence of text-to-image models, IET has expanded into new applications based on instructive commands. For example, EmoEdit [54] used GPT-4V to build emotion factor trees that map abstract emotions to specific visual elements and employed the InstructPix2Pix model to apply emotion-driven content and color adjustments to images.

Current methods primarily extract specific features, often focusing on certain visual elements or emotional cues, which can limit the depth of emotional expression. In contrast, our method broadly learns a variety of emotion-influencing features through the emotion-embedding network, mapping continuous emotional variations at the textual level. Additionally, our model can accept natural language prompts as input, allowing for a more intuitive and flexible way to generate emotionally expressive images.

2.3. Conditional Image Generation

Conditional image generation aims to produce images that align with specific input conditions, such as text, depth maps, or sketches. Early explorations in this field utilized Variational Autoencoders (VAEs) [14] and Generative Adversarial Networks (GANs) [9]. Currently, textual conditional image generation models based on denoising diffusion [12], such as Stable Diffusion [32, 35] and DALL-

E [3, 34], can generate exceptionally high-quality images. Besides, several studies have explored the use of other pieces of information as conditions for generation. The IP-adapter [56] integrates features from reference images through cross-attention, generating images consistent with attributes or identity. Techniques like Textual Inversion [8] and DreamBooth [36] can generate images in specific styles or domains by learning a concept. Models like ControlNet [58] and T2I-Adaptor [28] facilitate flexible conditional control using sketches, depth maps, and others.

However, there is limited research on the use of emotion as a condition. EmoGen [53] pioneered the generation of emotional image content (EIGC) by mapping emotional features to semantic features to create emotional images. Despite this, EmoGen struggles to understand natural language, limiting its capacity to effectively control specific content. Its reliance on discrete emotions also limits its practical applicability.

Our method bridges this gap by embedding continuous emotions into textual features, enabling image generation models to use both emotion and input prompts as conditions for creating emotional images.

3. Method

In this section, we introduce the technique details of *EmotiCrafter*. We begin with an overview of the proposed method, followed by an explanation of the network structure and key modules. Subsequently, we outline the training strategy. Finally, we describe the process of collecting and annotation of our dataset for network training.

3.1. Overview

As illustrated in Figure 2, our method generates emotional images I_{emo} from two inputs: text prompts describing the desired image content and a pair of V-A values (v, a) specifying the emotions. The process begins by encoding the input prompts into the prompt features f_n using a prompt encoder \mathcal{E} . These features then pass through an emotion-embedding network \mathcal{M} (Figure 2 (b.1)) to produce the emotional prompt features \hat{f}_e , embedded with emotion values (v, a) :

$$\hat{f}_e = \mathcal{M}(f_n|(v, a)). \quad (1)$$

Finally, the emotional prompt features are input via the cross-attention mechanism in the SDXL \mathcal{G} to generate the emotional images $I_{emo} = \mathcal{G}(\hat{f}_e)$. To enhance the emotional expressiveness of generated images, we develop a loss function (Figure 2 (b.2)) that optimizes the network training by considering the V-A distribution of the training data and enhancing the residuals between the features of the emotional prompts and neutral prompts, compelling that generated images convey the desired emotions and content. To facilitate our emotion-embedding network, we have compiled an

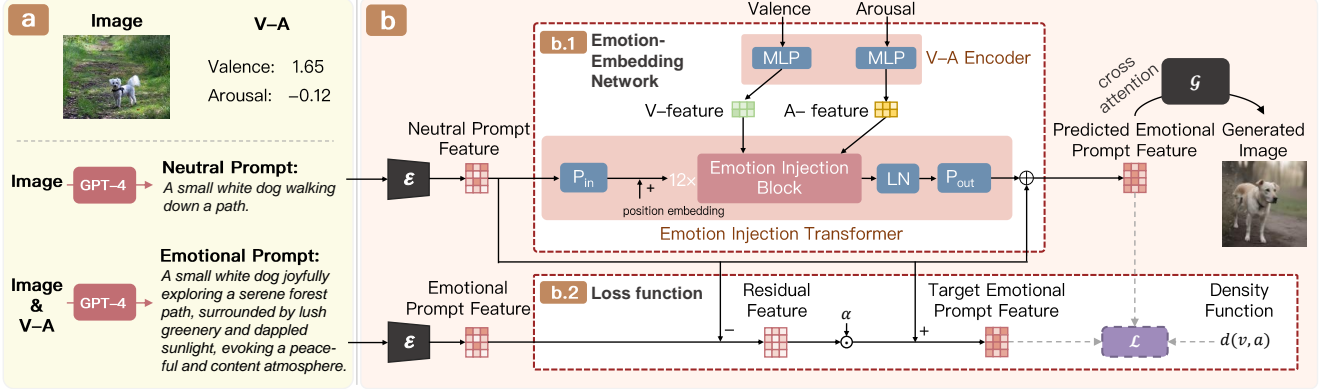


Figure 2. Overview of our method. Specifically, we take the following steps. (a) We collect an image dataset annotated with V-A values, neutral prompts, and emotional prompts. These prompts are then encoded into features by prompt encoder \mathcal{E} . (b) Next, we design (b.1) an emotion-embedding network \mathcal{M} to embed V/A values into textual features based on the transformer architecture, and (b.2) a specialized loss function to enhance the emotional resonance of generated images. The output of the mapping network serves as the condition for the image generation model \mathcal{G} to generate emotional images.

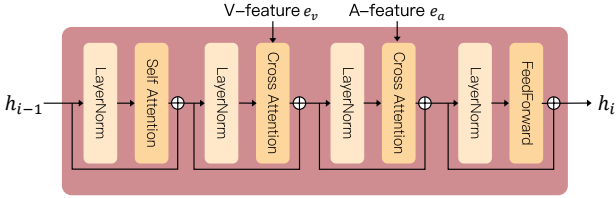


Figure 3. Structure of Emotion Injection Block. It accepts hidden state h_{i-1} as input and produces h_i as output. The V-feature e_v and A-feature e_a represent the emotional features, which are injected through the cross-attention module.

image dataset (Figure 2 (a)). This dataset pairs emotional images with both neutral prompts and emotional prompts, along with corresponding V-A values.

3.2. Emotion-Embedding Network

The emotion-embedding network \mathcal{M} takes a pair of V-A values and a neutral prompt feature as input and outputs the corresponding emotional prompt feature (Figure 2 (b.1)). In particular, it first employs a V-A encoder to convert the V-A values into feature vectors. After that, an emotion injection transformer network (structure modified from GPT-2 [33] in our implementation) is used to infuse these features into the neutral prompt feature. Here, the transformer helps with capturing and preserving the textual context of the neutral prompt while injecting emotional features.

V-A Encoder. The V-A Encoder transforms a pair of V-A values into emotional features using two separate multi-layer perceptrons (MLPs). The output V-features e_v and the A-features e_a are then transmitted into the emotion infusion process of the emotion injection transformer network.

Emotion Injection Transformer (EIT). The EIT is designed to effectively embed V/A-features into textual features through a modified GPT-2 architecture. The computing process of EIT consists of three steps: input projection,

emotion injection, and output projection. First, we project the input neutral prompt feature f_n into the transformer’s feature space:

$$h_0 = P_{\text{in}}(f_n) + \text{PE}, \quad (2)$$

where h_0 represents the initial hidden state, $P_{\text{in}}(\cdot)$ is a linear projection layer, and PE denotes positional embedding [41]. The core of EIT consists of 12 sequential **Emotion Injection Blocks (EIBs)** corresponding to 12 transformer blocks for emotion injection. Each block outputs a hidden state:

$$h_i = \text{EIB}(h_{i-1}, e_v, e_a), \quad i \in \{1, \dots, 12\} \quad (3)$$

where h_i is the output of the i -th EIB(\cdot). As shown in Figure 3, each EIB enhances the traditional transformer block through a cross-attention mechanism:

$$h'_i = \text{self-attn}(\text{LN}(h_{i-1})) + h_{i-1}, \quad (4)$$

$$h_i^{(v)} = \text{cross-attn}(\text{LN}(h'_i), e_v) + h'_i, \quad (5)$$

$$h_i^{(v,a)} = \text{cross-attn}(\text{LN}(h_i^{(v)}), e_a) + h_i^{(v)}, \quad (6)$$

$$h_i = \text{fnn}(\text{LN}(h_i^{(v,a)})) + h_i^{(v,a)}, \quad (7)$$

where h' , $h^{(v)}$, $h^{(v,a)}$ are the intermediate hidden variables; $\text{LN}(\cdot)$ is LayerNorm for normalization; $\text{self-attn}(\cdot)$ denotes self-attention, employed to capture context dependencies; $\text{cross-attn}(\cdot)$ is cross-attention for injecting e_v and e_a , and $\text{fnn}(\cdot)$ is a feed-forward network, which is used to introduce non-linear transformations to adapt to the complexity of the emotional embedding process. We also remove the causal mask typically used for next-token prediction from the original transformer model to fit our task. Finally, the output of the last (i.e., the 12th) injection block h_{12} is projected back to SDXL’s prompt feature space via P_{out} (a linear layer and a LayerNorm layer) to predict the residual between emotional and neutral prompt features, which represents a semantic

shift between emotional and neutral prompts:

$$\hat{f}_r = \text{P}_{\text{out}}(\text{LN}(h_{12})), \quad (8)$$

The final emotional prompt feature is obtained by adding this residual to the original neutral prompt feature:

$$\hat{f}_e = \hat{f}_r + f_n. \quad (9)$$

3.3. Loss Function

The above emotion embedding network is trained by minimizing the averaged expectation of the difference between the predicted emotional prompt feature $\hat{f}_e = \mathcal{M}(f_n|(v, a))$ and the scaled target emotional prompt feature f_e^t , using the loss function described in Equation 10.

$$\mathcal{L} = \frac{1}{n} \mathbb{E} \left(\frac{1}{d(v, a)} \|\hat{f}_e - f_e^t\|^2 \right) \quad (10)$$

where n is the number of feature elements; $\mathbb{E}(\cdot)$ denotes the expectation; $d(v, a)$ is a density function that describes the distribution of V-A values in the training sample.

To effectively embed emotions and address the challenges posed by the uneven distribution of V-A values in the dataset, this loss function incorporates two key strategies to improve the model’s performance:

Scaled Residual Learning. To better capture pronounced emotional changes in generated images, we enlarge the target residuals:

$$f_e^t = f_n + \alpha \underbrace{(f_e - f_n)}_{\text{residual feature}}, \quad (11)$$

where f_e is the emotional prompt feature, f_n is the neutral prompt feature, and α is a scale factor, we set its value to 1.5 based on the ablation study.

V-A Density Weighting. To mitigate the effects of the imbalanced distribution of the training samples, we weigh the loss inversely proportional to the density of training samples in the V-A space. The density is estimated using Kernel Density Estimation (KDE) [6] with a Gaussian kernel, denoted as $d(v, a)$:

$$d(v, a) = \frac{1}{n} \sum_{i=1}^n K_H((v, a) - (v_i, a_i)), \quad (12)$$

where K_H is a 2D Gaussian kernel with bandwidth H ; n is the number of training samples; (v_i, a_i) are the V-A values of the i -th training sample. The bandwidth H is selected using Silverman’s rule of thumb to provide optimal smoothing of the density estimation.

3.4. Dataset and Training

To train the emotion embedding network, an image caption dataset built on a set of annotated images is prepared. As

shown in Figure 2, given an image, a sample in our dataset is a 3-tuple that consists of (1) a pair of V-A values about the image labeled by human annotators and two prompts, i.e., (2) neutral prompt and (3) emotional prompt. Both prompts are automatically generated using GPT-4, taking the image as the input. In particular, the neutral [emotion] prompt describes the essential content of the image, whereas the emotional prompt describes the emotional information, such as the color, light, and texture, about the image.

In particular, we collected OASIS [19], EMOTIC [17], and FindingEmo [26] to gather enough images with human-annotated V-A values. These images offer a diverse range of scenes beyond just facial images. After cleaning and merging, we compiled a final dataset of 39,843 images with V-A annotations. We applied linear scaling to standardize the varying V-A scales across these datasets, adjusting the values to a uniform range of $[-3, 3]$ [26, 50]. Next, we applied prompt engineering to annotate the processed datasets with both neutral and emotional prompts, leveraging GPT-4’s vision capabilities to recognize essential content and express emotional nuances [7]. Please refer to the supplementary materials for further details.

The proposed emotion embedding network is trained based on two NVIDIA A800 GPUs using the above dataset. We utilize the AdamW [23] optimizer with a weight decay of $1e-5$ and a learning rate of $1e-3$. The training lasted for approximately 7 to 8 hours over a total of 200 epochs and 768 batch-size.

4. Experiments

In this section, we present both qualitative and quantitative comparisons, along with a user study and an ablation study, to evaluate the effectiveness of the proposed method.

4.1. Comparisons

To estimate the effectiveness of the proposed method, we built four baselines based on existing techniques.

Baselines. We built baselines for comparison via two strategies: (1) inject the emotion features directly into the image generation modules in the SDXL such as UNet; (2) use the emotion features to change the input text prompt that controls the content of the generated image (similar to the proposed method).

As a result, four different baselines were built: (1) *Cross Attention*: inject the emotion features (e_v, e_a) into the UNet in SDXL via its cross-attention mechanism based on IP-Adapter [56]; (2) *Time Embedding*: directly add emotion features (e_v, e_a) to the time embedding of the UNet in SDXL. (3) *Textual Inversion*: use the text inversion technique [8] to embed emotion features (e_v, e_a) into prompt templates with predefined emotion placeholders. (4) *GPT-4+SDXL (GPT-SD)*: use GPT-4 [1] to rewrite the input text according to (v, a) values to generate an emotional

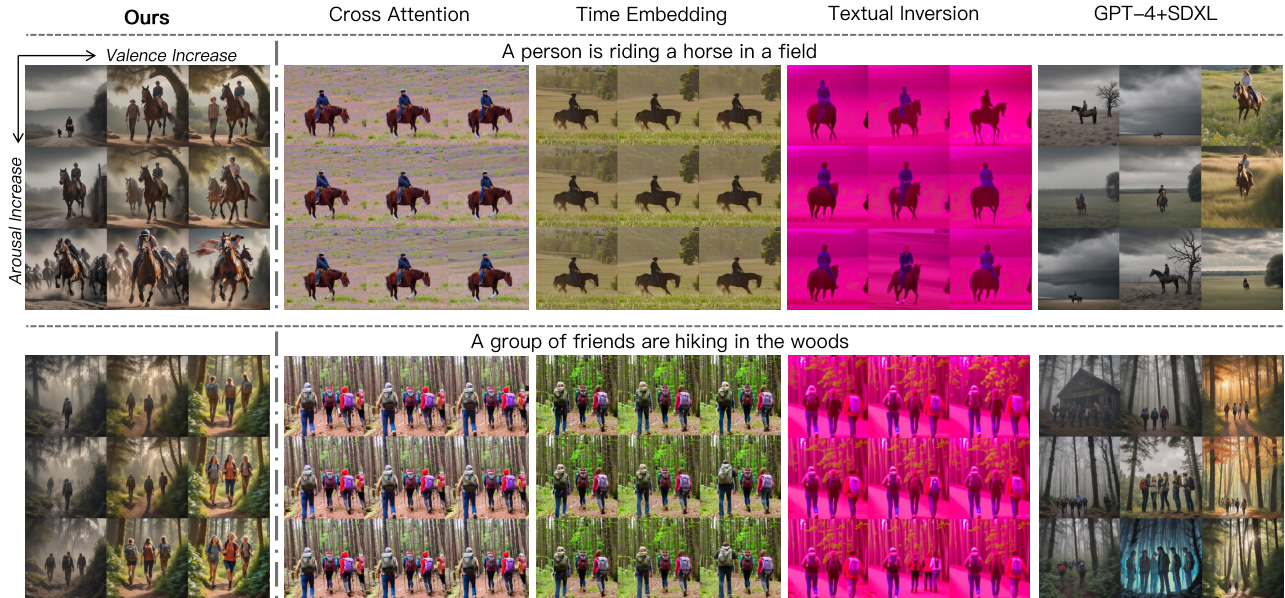


Figure 4. Qualitative comparisons with baselines. These images are generated at varying V-A values, specifically -1.5, 0, and 1.5. Only our approach and the GPT-4+SDXL successfully generate images that clearly reflect emotional variations. Notably, our results show enhanced continuity, indicating superior controllability over continuous V-A values compared to the GPT-4+SDXL.

SDXL prompt for image generation.

Qualitative Comparison. We evaluate the generated images based on three criteria: (1) the effectiveness of emotion embedding, (2) image-prompt similarity, and (3) the continuity of the image varies as V/A values change. Figure 4 illustrates that the baseline methods, Cross Attention, Time Embedding, and Textual Inversion, fail to reveal the continuous change of emotions. Notably, Textual Inversion tends to generate images with a persistent purple tint, which significantly limits its emotional expressiveness. Only our method and the GPT-4+SDXL successfully generate images that clearly reflect emotional variations. It also demonstrates that all methods generate content faithfully to the given prompts. For image continuity, we focus on comparing our method and GPT-4+SDXL, as they are the only two that successfully generate emotional variations. Our method shows enhanced continuity, indicating superior controllability over continuous V-A values. Figure 5 offers a more comprehensive comparison, revealing that our approach maintains continuity even under extreme V/A conditions. Conversely, GPT-4+SDXL displays noticeable discontinuities (e.g., in the V=3 column).

Quantitative Comparison. We compare our method against several baselines using the following metrics: (1) V/A -Error evaluates the absolute error between the predicted V/A values of the generated images and the input V/A values. (2) $CLIP$ Score [11] assesses the similarity between the input text and the generated images. (3) $CLIP$ -IQA [43] leverages a pre-trained CLIP model to evaluate image quality without requiring reference images.

(4) $LPIPS$ -Continuous utilizes the Learned Perceptual Image Patch Similarity [59] to measure the continuity of the change in image as V / A changes.

	A-Error ↓	V-Error ↓	CLIPScore ↑	CLIP-IQA ↑
Cross Attention	1.923±1.153	2.080±1.438	26.266±2.381	0.949±0.046
Time Embedding	1.941±1.168	2.031±1.348	26.566±2.125	0.786±0.164
Textual Inversion	1.958±1.188	1.923±1.170	22.346±3.594	0.370±0.111
GPT-4+SDXL	1.860±1.090	1.517±1.060	25.907±1.949	0.906±0.066
Ours	1.828±1.085	1.510±1.074	23.067±2.655	0.881±0.099

Table 1. Quantitative results comparing emotion accuracy, prompt fidelity, and image quality across different baselines (132 prompts \times 5 V/A values \times 25 images = 3,300 images per method). Our method achieves the highest performance in emotion accuracy, while maintaining comparable results in prompt fidelity and image quality, with a minor decrease due to the fact that altering emotional content will inherently affect semantic alignment.

As shown in Table 1, our method achieves the best (lowest) V/A -Error on average. Cross Attention and Time Embedding achieve the best (highest) $CLIP$ -IQA and $CLIP$ Score respectively. However, these methods fail to generate emotional images, as shown in Figure 4. Our method exhibits a slight decrease in $CLIP$ Score relative to the baselines. We believe this is due to the fact that altering emotional content will inherently affect semantic alignment. At the same time, $CLIP$ -IQA value shows that our method could generate high-quality images. Our method demonstrates superior continuity when compared to that of GPT-4 + SDXL (Table 2).

4.2. User Study

We conducted two user studies with 20 college students to evaluate the effectiveness of our method by comparing it to

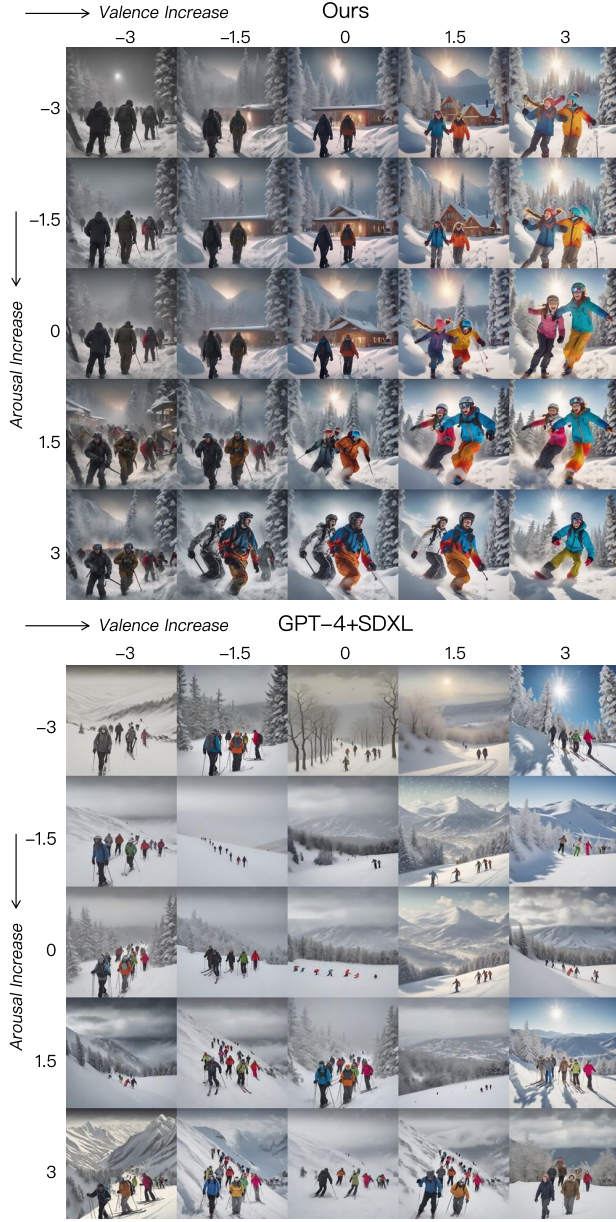


Figure 5. A more comprehensive comparison with the GPT-4+SDXL for the prompt “A group of people is skiing in a snow hill.” Our approach maintains continuity even under extreme V/A conditions. Conversely, GPT-4+SDXL displays noticeable discontinuities (e.g., in the V=3 column).

	Ours	GPT-4+SDXL
LPIPS-Continuous↓	0.220±0.064	0.361±0.059

Table 2. The continuity comparison between our method and GPT-4+SDXL (baseline).

GPT-4+SDXL (the baseline).

Experiment I. The first experiment tested whether the emotion represented by the generated images aligned with a human’s perception. To this end, two collections of im-

	Ours	GPT-4+SDXL
A-Ranking Consistency ↑	0.759±0.273	0.165±0.379
V-Ranking Consistency ↑	0.887±0.245	0.584±0.259
A-Error ↓	1.327±1.120	2.029±1.446
V-Error ↓	0.692±0.682	1.229±1.026
Emotion Consistency ↑	4.215±0.715	3.525±1.065
Emotion Smoothness ↑	4.240±0.828	3.195±1.163

Table 3. User study. Our method outperformed the baseline in all aspects.

ages were prepared respectively for testing the perception of A and V values. Each collection consists of 20 sets of images with 10 sets generated by our method and the other 10 sets generated by the baseline. Each set consisted of 5 images with different A or V values whose orders were randomized. The participants were asked to reorder these 5 images respectively based on the perceived intensity of V or A. Kendall’s $\tau_b \in [-1, +1]$ was computed to assess the alignment between the order given by participants and the ground truth order, where $\tau_b = 1$ indicated a full match of the orders. During the experiment, We also asked participants to use their perceived emotions to estimate and label the V and A values of each image. The absolute error between the results and the ground truth was calculated.

Experiment II. The second experiment was designed to test whether the generated images were able to reveal the contentious change of emotions (i.e., V-A values). To this end, we generated 20 sets of images (10 based on our method and the other 10 based on baseline). As shown in Figure 5, each set consists of 25 images generated based on V-A values gradually changed from -3 to +3. Participants were asked to rate each image set (using a 5-point Likert scale) regarding two aspects: (1) the consistency between the change of V-A values and the change of image content; (2) the smoothness of the change of the image content.

Analysis & Results. We conducted a Shapiro-Wilk test [38] to assess normality and applied the Wilcoxon Signed Rank test [46] to evaluate the significance of all the results. The results showed that our method outperformed the baseline in all aspects (Table 3) and showed a statistical significance regarding V/A Ranking, V/A Error, Consistency, and Smoothness (Figure 6).

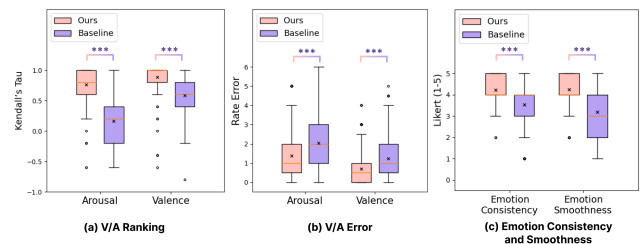


Figure 6. Significance test. (a) V/A Ranking: Kendall’s τ_b , (b) V/A Error: absolute error, (c) Emotion consistency, and Emotion smoothness. Significance levels: * $p < 0.05$, ** $p < 0.01$, *** $p < 0.001$

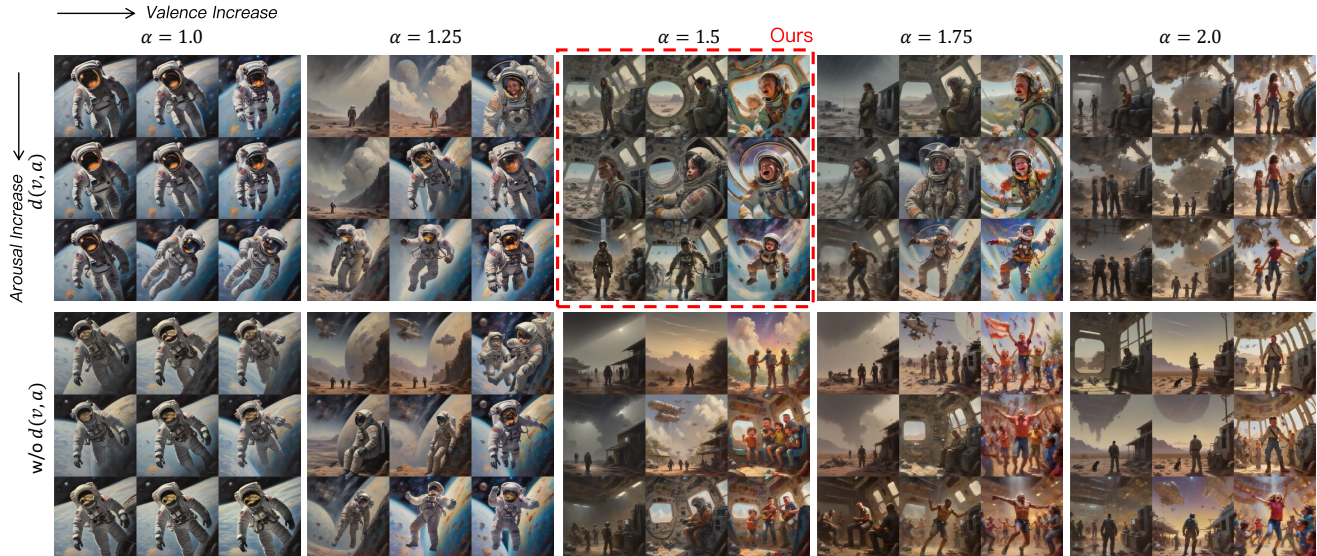


Figure 7. Ablation Study. Images are generated from the prompt “An oil painting shows an astronaut.” As α increases, image-prompt similarity decreases, while emotional variations increase. The usage of $d(a, v)$ enhances the accuracy of emotional changes in the generated images.

4.3. Ablation Study

We conducted ablation studies to estimate the effectiveness of the proposed loss function.

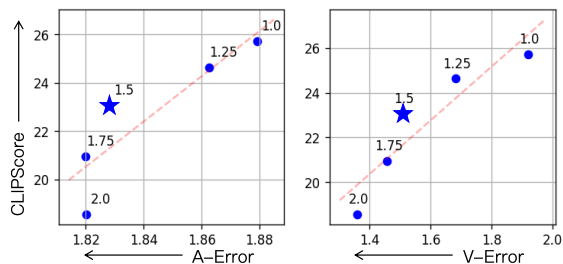


Figure 8. The effectiveness of the scaling factor α . The method with $\alpha = 1.5$ (★) surpasses the performance indicated by the regression line (---).

Effectiveness of the Scaling Factor α . We tested the changes of CLIPScore and V/A-Error while the scaling factor α varies. The results (Figure 8) showed that when α increased, both the CLIPScore and V/A-Error decreased (CLIPScore getting worse, V/A-Error getting better). This finding can also be observed from the examples shown in Figure 7. We set $\alpha = 1.5$ as a trade-off regarding the experiment results. However, users still can choose different α values to customize their output.

	A-Error ↓	V-Error ↓	CLIPScore ↑
Ours	1.828±1.085	1.510±1.074	23.067±2.655
w/o $d(v, a)$	1.829±1.083	1.546±1.082	21.977±0.066

Table 4. The effectiveness of $d(v, a)$.

Effectiveness of the Density Weighting $d(v, a)$. We compare our method with a variant that removed $d(v, a)$ from the training process. As shown in Table 4, incorporating $d(v, a)$ into the loss function positively affects both the CLIPScore and V/A-Error, which can also be easily found in Figure 7.

4.4. Discussion

Although our method achieved promising results, it still has some limitations that are worth mentioning: First, we observe that controlling image generation based on arousal is more challenging compared to valence. This aligns with prior research in visual emotion analysis, which has similarly reported that arousal is harder to predict, largely due to lower agreement among annotators when assessing arousal levels [26]; Second, our approach often generates images featuring human activities, even when such activities are not specified in the prompts. This tendency is likely attributable to the limited representation of non-human scenes in the training data and could be addressed by incorporating a greater variety of non-human scenarios into the dataset; Third, our method occasionally adjusts users’ input prompts to better align with the specified emotional prompts, resulting in a slight shift of the prompt meaning, thus effects the image generation. We believe this issue could be addressed by adding a term for semantic preserving in the loss function.

5. Conclusion

In this paper, we introduce a new task, i.e., continuous emotional image content generation (C-EICG), and present *EmotiCrafter*, a novel method for generating emotionally

expressive images based on continuous emotional values (Valence-Arousal). Specifically, we introduce an emotion-embedding network that integrates V-A values into textual features. Extensive experiments demonstrate the effectiveness of our approach, showing that it can reliably generate images that align with both user-provided prompts and specified emotions described by V-A values. We believe this work will catalyze further advancements in affective computing and image generation. To encourage future research, we will release our code and data, hoping it will inspire new developments in the field.

References

- [1] Josh Achiam, Steven Adler, Sandhini Agarwal, Lama Ahmad, Ilge Akkaya, Florencia Leoni Aleman, Diogo Almeida, Janko Altenschmidt, Sam Altman, Shyamal Anadkat, et al. Gpt-4 technical report. *arXiv preprint arXiv:2303.08774*, 2023. 5
- [2] Bitan Azari and Angelica Lim. Emostyle: One-shot facial expression editing using continuous emotion parameters. In *IEEE WACV*, pages 6385–6394, 2024. 2
- [3] James Betker, Gabriel Goh, Li Jing, Tim Brooks, Jianfeng Wang, Linjie Li, Long Ouyang, Juntang Zhuang, Joyce Lee, Yufei Guo, et al. Improving image generation with better captions. *Computer Science*. <https://cdn.openai.com/papers/dall-e-3.pdf>, 2(3):8, 2023. 3
- [4] Damian Borth, Rongrong Ji, Tao Chen, Thomas Breuel, and Shih-Fu Chang. Large-scale visual sentiment ontology and detectors using adjective noun pairs. In *ACM MM*, pages 223–232, 2013. 2
- [5] Hanna Chainay, George A Michael, Mélissa Vert-Pré, Lionel Landré, and Amandine Plasson. Emotional enhancement of immediate memory: Positive pictorial stimuli are better recognized than neutral or negative pictorial stimuli. *Advances in Cognitive Psychology*, 8(3):255, 2012. 2
- [6] Yen-Chi Chen. A tutorial on kernel density estimation and recent advances. *Biostatistics & Epidemiology*, 1(1):161–187, 2017. 5
- [7] Yasaman Etesam, Özge Nilay Yalçın, Chuxuan Zhang, and Angelica Lim. Contextual emotion recognition using large vision language models. *arXiv preprint arXiv:2405.08992*, 2024. 5
- [8] Rinon Gal, Yuval Alaluf, Yuval Atzmon, Or Patashnik, Amit Haim Bermano, Gal Chechik, and Daniel Cohen-or. An image is worth one word: Personalizing text-to-image generation using textual inversion. In *ICLR*, 2023. 3, 5
- [9] Ian Goodfellow, Jean Pouget-Abadie, Mehdi Mirza, Bing Xu, David Warde-Farley, Sherjil Ozair, Aaron Courville, and Yoshua Bengio. Generative adversarial networks. *Communications of the ACM*, 63(11):139–144, 2020. 3
- [10] Hatice Gunes, Björn Schuller, Maja Pantic, and Roddy Cowie. Emotion representation, analysis and synthesis in continuous space: A survey. In *IEEE FG*, pages 827–834, 2011. 2
- [11] Jack Hessel, Ari Holtzman, Maxwell Forbes, Ronan Le Bras, and Yejin Choi. Clipscore: A reference-free evaluation metric for image captioning. In *EMNLP*, pages 7514–7528, 2021. 6
- [12] Jonathan Ho, Ajay Jain, and Pieter Abbeel. Denoising diffusion probabilistic models. *NeurIPS*, 33:6840–6851, 2020. 3
- [13] Stephen Khor Wen Hwooi, Alice Othmani, and Aznul Qalid Md. Sabri. Deep learning-based approach for continuous affect prediction from facial expression images in valence-arousal space. *IEEE Access*, 10:96053–96065, 2022. 2
- [14] Diederik P Kingma. Auto-encoding variational bayes. *arXiv preprint arXiv:1312.6114*, 2013. 3
- [15] Dimitrios Kollias. Abaw: Valence-arousal estimation, expression recognition, action unit detection & multi-task learning challenges. In *CVPR*, pages 2328–2336, 2022. 2
- [16] Ronak Kosti, Jose M. Alvarez, Adria Recasens, and Agata Lapedriza. Emotion recognition in context. In *CVPR*, 2017. 2
- [17] Ronak Kosti, Jose M. Alvarez, Adria Recasens, and Agata Lapedriza. Emotion recognition in context. In *CVPR*, pages 1667–1675, 2017. 5
- [18] Philip A Kragel, Marianne C Reddan, Kevin S LaBar, and Tor D Wager. Emotion schemas are embedded in the human visual system. *Science advances*, 5(7):eaaw4358, 2019. 2, 3
- [19] Benedek Kurdi, Shayn Lozano, and Mahzarin R Banaji. Introducing the open affective standardized image set (oasis). *Behavior research methods*, 49:457–470, 2017. 5
- [20] Angela Y Lee and Brian Sternthal. The effects of positive mood on memory. *Journal of consumer research*, 26(2):115–127, 1999. 2
- [21] Jiansheng Li, Chuanlan Luo, Qi Zhang, and Rustam Shadiev. Can emotional design really evoke emotion in multimedia learning? *International Journal of Educational Technology in Higher Education*, 17:1–18, 2020. 2
- [22] Da Liu, Yaxi Jiang, Min Pei, and Shiguang Liu. Emotional image color transfer via deep learning. *Pattern Recognition Letters*, 110:16–22, 2018. 3
- [23] I Loshchilov. Decoupled weight decay regularization. *arXiv preprint arXiv:1711.05101*, 2017. 5
- [24] Olga Megalaki, Ugo Ballenghein, and Thierry Baccino. Effects of valence and emotional intensity on the comprehension and memorization of texts. *Frontiers in Psychology*, 10:179, 2019. 2
- [25] Liyu Meng, Yuchen Liu, Xiaolong Liu, Zhaopei Huang, Yuan Cheng, Meng Wang, Chuanhe Liu, and Qin Jin. Multimodal emotion estimation for in-the-wild videos. *arXiv preprint arXiv:2203.13032*, 2022. 2
- [26] Laurent Mertens, Elahe’ Yargholi, Hans Op de Beeck, Jan Van den Stock, and Joost Vennekens. Findingemo: An image dataset for emotion recognition in the wild. *arXiv preprint arXiv:2402.01355*, 2024. 2, 3, 5, 8
- [27] Ali Mollahosseini, Behzad Hasani, and Mohammad H. Mahoor. Affectnet: A database for facial expression, valence, and arousal computing in the wild. *IEEE Transactions on Affective Computing*, 10(1):18–31, 2019. 2
- [28] Chong Mou, Xintao Wang, Liangbin Xie, Yanze Wu, Jian Zhang, Zhongang Qi, Ying Shan, and Xiaohu Qie. T2i-adapter: Learning adapters to dig out more controllable

- ability for text-to-image diffusion models. *arXiv preprint arXiv:2302.08453*, 2023. 3
- [29] Chanjong Park and In-Kwon Lee. Emotional landscape image generation using generative adversarial networks. In *ACCV*, 2020. 2
- [30] Monika Pawłowska and Ewa Magier-Łakomy. The influence of emotional and non-emotional concepts activation on information processing and unintentional memorizing. *Polish Psychological Bulletin*, 2011. 2
- [31] Kuan-Chuan Peng, Tsuhan Chen, Amir Sadovnik, and Andrew C Gallagher. A mixed bag of emotions: Model, predict, and transfer emotion distributions. In *CVPR*, pages 860–868, 2015. 3
- [32] Dustin Podell, Zion English, Kyle Lacey, Andreas Blattmann, Tim Dockhorn, Jonas Müller, Joe Penna, and Robin Rombach. SDXL: Improving latent diffusion models for high-resolution image synthesis. In *ICLR*, 2024. 2, 3
- [33] Alec Radford, Jeffrey Wu, Rewon Child, David Luan, Dario Amodei, Ilya Sutskever, et al. Language models are unsupervised multitask learners. *OpenAI blog*, 1(8):9, 2019. 4
- [34] Aditya Ramesh, Prafulla Dhariwal, Alex Nichol, Casey Chu, and Mark Chen. Hierarchical text-conditional image generation with clip latents. *arXiv preprint arXiv:2204.06125*, 1(2):3, 2022. 3
- [35] Robin Rombach, Andreas Blattmann, Dominik Lorenz, Patrick Esser, and Björn Ommer. High-resolution image synthesis with latent diffusion models. In *CVPR*, pages 10684–10695, 2022. 3
- [36] Nataniel Ruiz, Yuanzhen Li, Varun Jampani, Yael Pritch, Michael Rubinstein, and Kfir Aberman. Dreambooth: Fine tuning text-to-image diffusion models for subject-driven generation. In *CVPR*, pages 22500–22510, 2023. 3
- [37] James A Russell. A circumplex model of affect. *Journal of personality and social psychology*, 39(6):1161, 1980. 2
- [38] S Shaphiro and MBBJ Wilk. An analysis of variance test for normality. *Biometrika*, 52(3):591–611, 1965. 7
- [39] Antoine Toisoul, Jean Kossaifi, Adrian Bulat, Georgios Tzimiropoulos, and Maja Pantic. Estimation of continuous valence and arousal levels from faces in naturalistic conditions. *Nature Machine Intelligence*, 3(1):42–50, 2021. 2
- [40] Chai M Tyng, Hafeez U Amin, Mohamad NM Saad, and Aamir S Malik. The influences of emotion on learning and memory. *Frontiers in psychology*, 8:235933, 2017. 2
- [41] Ashish Vaswani. Attention is all you need. *NeurIPS*, 2017. 4
- [42] Manuelde Vega. The representation of changing emotions in reading comprehension. *Cognition & emotion*, 10(3):303–322, 1996. 2
- [43] Jianyi Wang, Kelvin CK Chan, and Chen Change Loy. Exploring clip for assessing the look and feel of images. In *AAAI*, pages 2555–2563, 2023. 6
- [44] Yan Wang, Wei Song, Wei Tao, Antonio Liotta, Dawei Yang, Xinlei Li, Shuyong Gao, Yixuan Sun, Weifeng Ge, Wei Zhang, et al. A systematic review on affective computing: Emotion models, databases, and recent advances. *Information Fusion*, 83:19–52, 2022. 2
- [45] Shuchen Weng, Peixuan Zhang, Zheng Chang, Xinlong Wang, Si Li, and Boxin Shi. Affective image filter: Reflecting emotions from text to images. In *ICCV*, pages 10810–10819, 2023. 3
- [46] Frank Wilcoxon. Individual comparisons by ranking methods. In *Breakthroughs in statistics: Methodology and distribution*, pages 196–202. Springer, 1992. 7
- [47] Weizhen Xie and Weiwei Zhang. Negative emotion enhances mnemonic precision and subjective feelings of remembering in visual long-term memory. *Cognition*, 166:73–83, 2017. 2
- [48] Chao Xu, Junwei Zhu, Jiangning Zhang, Yue Han, Wenqing Chu, Ying Tai, Chengjie Wang, Zhifeng Xie, and Yong Liu. High-fidelity generalized emotional talking face generation with multi-modal emotion space learning. In *CVPR*, pages 6609–6619, 2023. 2
- [49] Liwen Xu, Zhengtao Wang, Bin Wu, and Simon Lui. Mdan: Multi-level dependent attention network for visual emotion analysis. In *CVPR*, pages 9479–9488, 2022. 2
- [50] Xu Xu, Jiayin Li, and Huilin Chen. Valence and arousal ratings for 11,310 simplified chinese words. *Behavior research methods*, 54(1):26–41, 2022. 5
- [51] Dingkan Yang, Shuai Huang, Shunli Wang, Yang Liu, Peng Zhai, Liuzhen Su, Mingcheng Li, and Lihua Zhang. Emotion recognition for multiple context awareness. In *ECCV*, pages 144–162, Cham, 2022. Springer Nature Switzerland. 2
- [52] Jufeng Yang, Dongyu She, and Ming Sun. Joint image emotion classification and distribution learning via deep convolutional neural network. In *IJCAI*, pages 3266–3272, 2017. 2
- [53] Jingyuan Yang, Jiawei Feng, and Hui Huang. Emogen: Emotional image content generation with text-to-image diffusion models. In *CVPR*, pages 6358–6368, 2024. 2, 3
- [54] Jingyuan Yang, Jiawei Feng, Weibin Luo, Dani Lischinski, Daniel Cohen-Or, and Hui Huang. Emoedit: Evoking emotions through image manipulation. *arXiv preprint arXiv:2405.12661*, 2024. 3
- [55] Xiaocui Yang, Shi Feng, Daling Wang, and Yifei Zhang. Image-text multimodal emotion classification via multi-view attentional network. *IEEE Transactions on Multimedia*, 23: 4014–4026, 2021. 2
- [56] Hu Ye, Jun Zhang, Sibio Liu, Xiao Han, and Wei Yang. Ip-adapter: Text compatible image prompt adapter for text-to-image diffusion models. *arXiv preprint arXiv:2308.06721*, 2023. 3, 5
- [57] Ligang Zhang, Dian Tjondronegoro, and Vinod Chandran. Representation of facial expression categories in continuous arousal-valence space: feature and correlation. *Image and Vision Computing*, 32(12):1067–1079, 2014. 2
- [58] Lvmin Zhang, Anyi Rao, and Maneesh Agrawala. Adding conditional control to text-to-image diffusion models. In *ICCV*, pages 3836–3847, 2023. 3
- [59] Richard Zhang, Phillip Isola, Alexei A Efros, Eli Shechtman, and Oliver Wang. The unreasonable effectiveness of deep features as a perceptual metric. In *CVPR*, pages 586–595, 2018. 6
- [60] Zixing Zhang, Liyizhe Peng, Tao Pang, Jing Han, Huan Zhao, and Björn W Schuller. Refashioning emotion recognition modelling: The advent of generalised large models.

IEEE Transactions on Computational Social Systems, 2024.

2

- [61] Sicheng Zhao, Yue Gao, Xiaolei Jiang, Hongxun Yao, Tat-Seng Chua, and Xiaoshuai Sun. Exploring principles-of-art features for image emotion recognition. In *ACM MM*, pages 47–56, 2014. 2
- [62] Sicheng Zhao, Hongxun Yao, and Xiaolei Jiang. Predicting continuous probability distribution of image emotions in valence-arousal space. In *ACM MM*, page 879–882, New York, NY, USA, 2015. Association for Computing Machinery. 2
- [63] Sicheng Zhao, Xingxu Yao, Jufeng Yang, Guoli Jia, Guiguang Ding, Tat-Seng Chua, Björn W. Schuller, and Kurt Keutzer. Affective image content analysis: Two decades review and new perspectives. *IEEE TPAMI*, 44(10):6729–6751, 2022. 2
- [64] Siqi Zhu, Chunmei Qing, Canqiang Chen, and Xiangmin Xu. Emotional generative adversarial network for image emotion transfer. *Expert Systems with Applications*, 216:119485, 2023. 3
- [65] Siqi Zhu, Chunmei Qing, Canqiang Chen, and Xiangmin Xu. Emotional generative adversarial network for image emotion transfer. *Expert Systems with Applications*, 216:119485, 2023. 3